Since January 2020 Elsevier has created a COVID-19 resource centre with free information in English and Mandarin on the novel coronavirus COVID-19. The COVID-19 resource centre is hosted on Elsevier Connect, the company's public news and information website.

International Journal of Biological Macromolecules 213 (2022) 1007–1017

Contents lists available at ScienceDirect

International Journal of Biological Macromolecules

journal homepage: www.elsevier.com/locate/ijbiomac

Production and characterization of chimeric SARS-CoV-2 antigens based on the capsid protein of cowpea chlorotic mottle virus

Claudia Almendárez-Rodriguez [a,b], Karla I. Solis-Andrade [b], Dania O. Govea-Alonso [b], Mauricio Comas-Garcia [b,c,d,*], Sergio Rosales-Mendoza [a,b,*]

[a] Facultad de Ciencias Químicas, Universidad Autónoma de San Luis Potosí, Av. Dr. Manuel Nava 6, SLP 78210, Mexico
[b] Sección de Biotecnología, Centro de Investigación en Ciencias de la Salud y Biomedicina, Universidad Autónoma de San Luis Potosí, Av. Sierra Leona 550, Lomas 2ª. Sección, San Luis Potosí 78210, Mexico
[c] Sección de Microscopía de Alta Resolución, Centro de Investigación en Ciencias de la Salud y Biomedicina, Universidad Autónoma de San Luis Potosí, Av. Sierra Leona 550, Lomas 2ª. Sección, San Luis Potosí 78210, Mexico
[d] Facultad de Ciencias, Universidad Autónoma de San Luis Potosí, Av. Parque Chapultepec 1570, 78210 San Luis, S.L.P., San Luis Potosí 78210, Mexico

ARTICLE INFO

Keywords:
Humoral response
Plant virus
Chimeric protein

ABSTRACT

The COVID-19 pandemic has highlighted the need for new vaccine platforms to rapidly develop solutions against emerging pathogens. In particular, some plant viruses offer several advantages for developing subunit vaccines, such as high expression rates in *E. coli*, high immunogenicity and safety, and absence of pre-immunity that could interfere with the vaccine's efficacy. Cowpea chlorotic mottle virus (CCMV) is a model system that has been extensively characterized, with key advantages for its use as an epitope carrier. In the present study, three relevant epitopes from the SARS-CoV-2 Spike protein were genetically inserted into the CCMV CP and expressed in *E. coli* cultures, resulting in the CCMV1, CCMV2, and CCMV3 chimeras. The recombinant CP mutants were purified from the formed inclusion bodies and refolded, and their immunogenicity as a subunit vaccine was assessed in BALB/c mice. The three mutants are immunogenic as they induce high IgG antibody titers that recognize the recombinant full-length S protein. This study supports the application of CCMV CP as an attractive carrier for the clinical evaluation of vaccine candidates against SARS-CoV-2. Furthermore, it suggests that VLPs assembled from these chimeric proteins could result in antigens with better immunogenicity.

1. Introduction

The Severe Acute Respiratory Syndrome Coronavirus (SARS-CoV-2) is the etiological agent of the Coronavirus 19 Disease (COVID-19), originated in the province of Wuhan, China, in 2019 [1]; which rapidly imposed a considerable burden on public health, disrupted the global economy, and almost all social activities [2]. Nonetheless, this pandemic helped to develop novel vaccine platforms and technologies that seemed far from being approved for human health purposes [3]. In particular, the development of vaccines is the most crucial approach to combat this pandemic resulting in an unprecedented, accelerated development of several candidates.

Neutralizing antibodies and/or T-cell immune responses are the basis for providing immunoprotection against SARS-CoV-2, with the Spike (S) protein being the primary target immunogen. Based on studies with SARS-CoV and MERS-CoV, it was rapidly identified that the "Receptor Binding Domain" (RBD) in the S1 domain of the S protein is the primary site for the induction of neutralizing antibodies [4].

Coronaviruses have the most stable genome amongst single-stranded RNA (ssRNA) viruses [5]. Their mutation rate is higher than double-stranded DNA viruses [6] but lower than most ssRNA viruses. Highly pathogenic coronaviruses can mutate to generate a series of SARS-CoV-2 variants of concern (VOC). VOCs are defined as those that have genetic changes that are predicted, or known, to affect viral characteristics such as transmissibility, disease severity, and immune escape [7]. Amongst all VOC, the WHO has cataloged the Delta variant (lineage B.1.617.2 y AY) and omicron variant (lineage B.1.1.529 y BA) as the most concerning ones; there are key point mutations that help the virus to escape the neutralizing antibodies from recovered patients [8] and the approved vaccines.

* Corresponding author at: Centro de Investigación en Ciencias de la Salud y Biomedicina, Universidad Autónoma de San Luis Potosí, Av. Sierra Leona 550, Lomas 2ª. Sección, San Luis Potosí 78210, Mexico.
E-mail addresses: mauricio.comas@uaslp.mx (M. Comas-Garcia), rosales.s@uaslp.mx (S. Rosales-Mendoza).

https://doi.org/10.1016/j.ijbiomac.2022.06.021
Received 6 April 2022; Received in revised form 2 June 2022; Accepted 5 June 2022
Available online 8 June 2022

Several platforms have been explored for the development of vaccines against SARS-CoV-2. In ascending order of frequency as approved technologies, there are vaccines based on: protein subunits, inactivated viruses, mRNA encapsulated in liposomes, and adenoviral vectors. However, other technologies exist in pre-clinical and clinical stages, such as virus-like particles, replicating viral vectors, and live attenuated viruses [9].

Although most SARS-CoV-2 vaccines are currently used worldwide under authorizations for emergency use, it is clear that new platforms should be implemented to guarantee global vaccination as well as a rapid response against new VOCs, especially those with the capacity to evolve into variants of concern with higher transmissibility and immune evasion. According to the WHO database, subunit vaccines are the most prominent candidates under clinical development. These vaccines have remarkable advantages: they do not contain any replicative components of the pathogen that could cause an infection in case of poor inactivation or reverberant mutations that turn the virus infectious. Furthermore, subunit vaccines can offer the induction of immune responses focused on specific protein domains or epitopes from the pathogen, which could ultimately optimize vaccines' rational design [10]. On the other hand, the side effects are less common because subunit vaccines contain only the target antigen. On the other hand, such simplification is also often associated with poor immunogenicity; hence to overcome this limitation, these formulations are often supplemented with adjuvants [11].

Plant viruses are attractive platforms for gene and drug delivery and the presentation of immunogenic peptides [12]. Amongst all the plant viruses used in biotechnology, cowpea chlorotic mottle virus (CCMV) is probably one of the most studied RNA viruses: it can be reconstituted from either purified components or ectopically expressed recombinant proteins [13]. On the one hand, it can be assembled in the absence of nucleic acids in a wide range of macromolecular arranges [14]. On the other hand, it can package almost any flexible and negatively charged polymer (e.g., oligos, ssRNA, and polymers). The CCMV capsid protein (CP) is a promising antigen carrier for vaccine design; several studies have shown its safety in vivo in several test animals [15] and have been explored for other biomedical applications such as drug delivery, imaging, and tumor therapy [16]. Recombinant CCMV CP has been efficiently produced in *E. coli* as a host [17,18], resulting in high yields that have supported its assessment in biophysical studies and nanotechnology and biomedical applications [19]. This system offers the advantage that the CP can be genetically and/or chemically modified to expose novel chemical moieties or antigens, which can then be presented either as a dimeric protein or as a virion (empty or filled with RNA). Furthermore, unlike adenoviral vectors, it does not impose limitations in terms of preexisting immunity, given that it is a plant virus whose reservoir does not include humans, and thus vaccinees lack of anti-carrier antibodies at the priming phase.

In the present study, the CCMV CP was genetically modified to generate three different mutant CPs decorated with SARS-CoV-2 linear epitopes. The CP was expressed in *E. coli* and purified under non-assembling conditions that promote the protein in a dimeric state. The chimeric CCMV CP was explored as an initial approach to obtain highly immunogenic proteins capable of presenting epitopes from the RBD to the immune system. The humoral immunogenicity of the three chimeric CCMV CPs was tested in BALB/c mice.

2. Methods and materials

2.1. Plasmid design

The CCMV CP was used as a scaffold to display SARS-CoV-2 epitopes. We designed three chimeric proteins to display epitopes of the SARS-CoV-S protein: CCMV1 ($S_{462\text{-}500}$), CCMV2 ($S_{505\text{-}522}$), and CCMV3 ($S_{439\text{-}460}$). The S sequences were inserted between amino acids 164 and 165, that is, at the loop between βH-βI [16]. The sequence of the wild-type CCMV CP (Gene Bank: M28818.1A) was used as a scaffold. All four genes were synthesized by Gene Script, INC. The synthetic genes were codon-optimized for *E. coli* by the vendor and cloned into the vector pET-15b at the NdeI/BamHI restriction sites and with a His-Tag at the N-termini. These plasmids have an ampicillin-resistant gene.

2.2. Structure prediction for chimeric proteins

The insertion site of the SARS-CoV-2 epitopes into the CCMV CP was decided by modeling the chimeric protein using the ProMod3 modeling engine from the Swiss-Model homology modeling server (version 1.0.0; https://swissmodel.expasy.org) using the structure of the native CP of CCMV (PDB: 1za7.1) as a template. The insertion site was selected as that disturbed the least the tertiary structure of the modeled chimeric protein for the native CP. This analysis was performed with the UCSF Chimera X molecular modeling program.

2.3. E. coli transformation and preliminary protein expression assays

Chemically competent *Rosetta* DE3 *E. coli cells* were transformed with the expression vectors and plated Agar-Luria Broth (LB) plates supplemented with ampicillin (50 mg/mL) and chloramphenicol (40 mg/mL) and incubated overnight at 37 °C. Several colonies were selected and propagated in LB media with the proper antibiotics to assess protein expression. A pre-inoculum was generated for each of the selected colonies by inoculating them in 50 mL of LB medium supplemented with 40 mg/mL chloramphenicol and 50 mg/mL ampicillin, followed by incubation at 37 °C for 24 h at 150 rpm. The inoculums were 10-fold diluted in a flask containing 2YT medium (16 g/L Bacto Tryptone, 10 g/L Yeast extract, 5 g/L NaCl, pH 7.0) supplemented with the proper antibiotics, and grown at 37 °C until the OD_{600} was between 0.6 and 0.8. An aliquot of the culture was taken before protein induction as a negative control. Protein expression was subsequently induced by adding 0.1 mM IPTG followed by incubation at 28 °C for a 4 h-period. The cells were centrifugated at 6500 RCF for 15 min at 4 °C and stored at −80 °C until further processing.

2.4. Protein extraction and SDS-PAGE analysis

The biomass recovered from expression experiments was stored at −80 °C, thawed and resuspended in 2.5 mL of disassembly buffer (10 mM imidazole, 300 mM NaCl, 50 mM Na_2HPO_4, pH 8.0). The cells were subsequently lysed by sonication using a sonicator at 70 % amplitude (Sonics Vibra Cell, CT, USA) on ice over for 10 min period comprising 10 s-pulses followed by 10 s-off periods and an aliquot stored for further analysis (total protein). The lysate was centrifuged at 6500 RCF for 15 min, and the supernatant (soluble fraction) was separated from the pellet (insoluble fraction). The pellet was resuspended in 2.5 mL of disassembly buffer.

The expression profile was determined by SDS-PAGE. The pre-induction fraction, the total protein extract, and the soluble and insoluble protein fractions were analyzed in 12 % SDS-PAGE gel. Each lane was loaded with 30 μL of the corresponding sample previously mixed with 5 μL of 5× loading buffer and boiled for 5 min at 98 °C. The gels were run at 120 V for 1 h and stained with a Coomassie blue solution.

2.5. Purification of CCMV chimeras

The colonies that exhibited the best expression profile were used to express the desired proteins in 250 mL of LB with the proper antibiotics following the same conditions as the initial expression conditions (see above). The bacterial pellet was resuspended in 4 mL of 20 mM Tris-HCl pH 8.0 and subsequently disrupted by sonication at a 70 % amplitude for 1min on ice (10 s-pulses followed by 10 s-off periods). The lysate was centrifuged for 10 min at 6500 RCF and 4 °C. The pellet was resuspended in 3 mL of cold denaturing buffer (2 M urea, 20 mM Tris-HCl, 0.5 M NaCl, 2 % Triton™ X-100 pH 8.0) and sonicated as previously described.

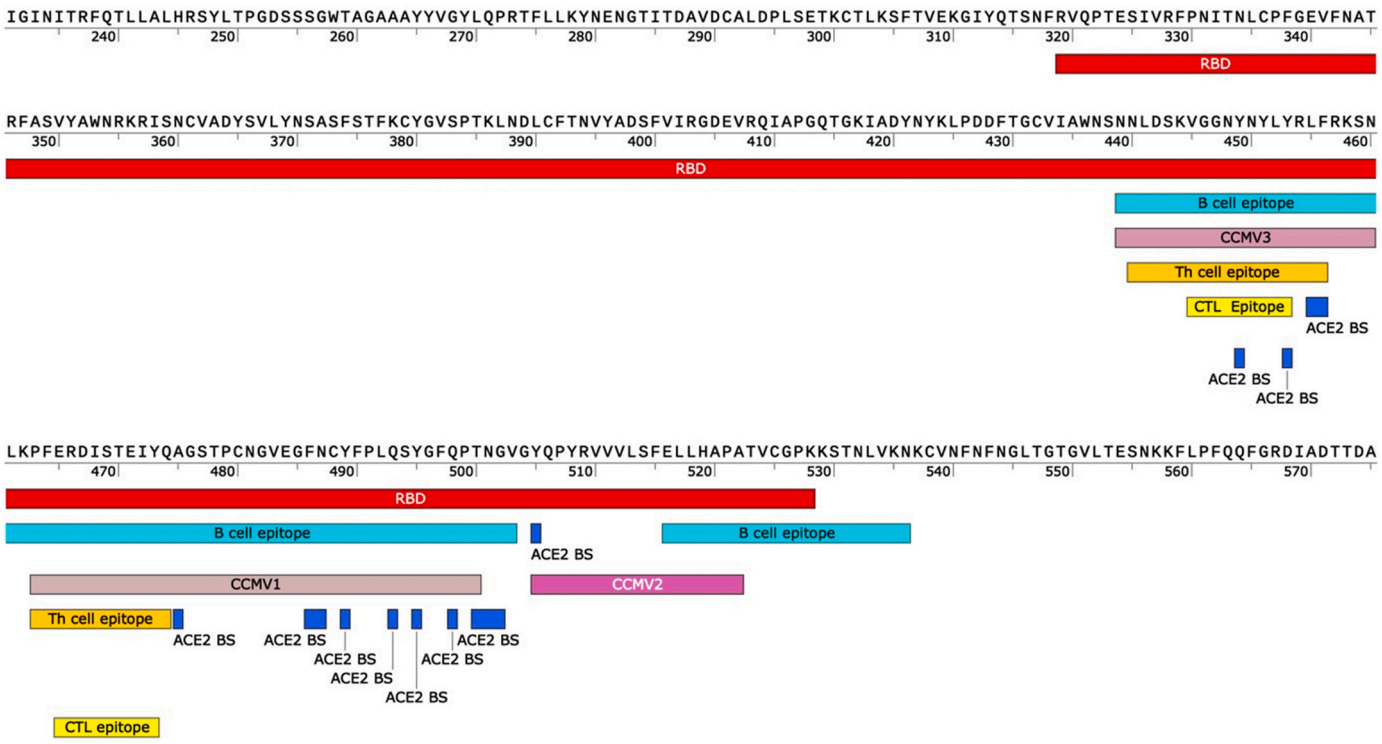

Fig. 1. Localization of the target epitopes. A segment of the primary sequence of the SARS-CoV-2 s protein from amino acids 231 to 575 that indicate the localization of the SARS-CoV-2 epitopes in the "Receptor Binding Domain" (RBD) inserted into the three chimeric CCMV capsid proteins: CCMV 1 ($S_{462–500}$), 2 ($S_{505–522}$), and 3 ($S_{439–460}$). These epitopes contain binding ACE-2 binding sites (BS), B, Th, and CTL epitopes.

The solution was centrifuged at 6500 RCF for 10 min at 4 °C. The pellet was washed with the denaturing buffer and centrifuged. The pellet was resuspended in 5 mL 20 mM Tris-HCl, 0.5 M NaCl, 5 mM imidazole, 6 M guanidine hydrochloride, and 1 mM 2-mercaptoethanol, pH 8.0. The solution was stirred with a magnetic bar for 60 min at room temperature and subsequently centrifuged for 15 min at 6500 RCF. The solubilized protein was incubated with 1 mL of His Pur™ Ni-NTA Resin for 1 h at 4 °C under constant agitation in an orbital shaker. The sample was centrifuged at 4500 RCF for 5 min at 4 °C, and the supernatant was kept for further analysis. The resin was washed several times with 10 mL of a Ni-NTA denaturing buffer (20 mM Tris-HCl, 0.5 M NaCl, 20 mM imidazole, 1 mM 2-mercaptoethanol, 6 M urea, pH 8.0.). The protein was refolded while bound to the resin using a linear 6–0 M urea gradient. Each wash consisted of a 5 min-incubation, followed by a centrifugation step (5 min at 4500 RCF). The resin was subsequently washed with 3 mL of buffer containing 20 mM imidazole, 300 mM NaCl, 50 mM Na_2HPO_4, pH 8.0, and the elution of the target protein was induced by washing the resin 1 mL of buffer containing 500 mM imidazole, 300 mM NaCl, 50 mM Na_2HPO_4, pH 8.0. The elution step was repeated twice. The protein content at each step was analyzed by SDS-PAGE, as indicated in the previous sections.

2.6. Immunoblot

The protein extracts (30 μL samples) were loaded into an SDS-PAGE 12 % and ran as previously mentioned, and the proteins were transferred into Nitrocellulose Membrane BIO-RAD™ for1 h at 500 mA. The membrane was blocked overnight with a 5 % milk solution at 4 °C, followed by three 10 min-washes with PBS-Tween. Primary labeling was performed overnight at 4 °C using an anti-$S_{461–493}$ hyperimmune obtained in sheep (dilution 1:10,000) [20]. The membrane was subjected to three 10 min-washes with PBS-Tween before the addition of a donkey anti-sheep antibody conjugated with horseradish peroxidase (1:10,000 dilution, Sigma-Aldrich, St. Louis, MO) followed by incubation for 2 h at room temperature. After three 10 min-washes with PBS-Tween, the membrane was treated with peroxidase chemiluminescent substrates and developed on photosensitive screens for 15 min in a dark room.

2.7. Immunization assay

BALB/c mice were used for the immunization assays, which were approved by the institutional ethics committee (CEID-2020-07R1). Mice were 8 to 10 weeks old and randomly divided into nine groups ($n = 4$). Mice were subjected to an immunization scheme comprising the administration of three subcutaneous doses (100 μL) on the back on days 0, 14, and 21. The experimental groups are: group 1 – PBS, group 2–10 μg of CCMV1 + PBS, group 3–10 μg of CCMV1 + $Al(OH)_3$, group 4–10 μg of WT CCMV CP, group 5–10 μg of CCMV2 + PBS, group 6–10 μg of CCMV2 + $Al(OH)_3$, group 7–10 μg of CCMV3 + PBS, group 8–10 μg of CCMV3 + $Al(OH)_3$, and group 9–25 μg of CCMV1 + CCMV2 + CCMV3 + $Al(OH)_3$. Blood samples from the tail were taken on days 0, 13, 20, 39, 56, and 159. The serum was separated from total blood by centrifugation for 10 min at 5000 RPM and kept at −20 °C until further use. The Al $(OH)_3$ adjuvant (G biosciences, cat no. 786–1215) was used at a 1:5 ratio.

2.8. Enzyme linked immunosorbent assay (ELISA)

Ninety-six-well polystyrene plates were coated with the different target antigens: a synthetic peptide containing amino acids 461–493 of the S protein from the Wuhan isolate, the full-length S protein from the Wuhan sequence (SinoBiological Inc. cat. No. 40589-V08H4), the full-length S protein from the Delta variant (SinoBiological Inc. cat. No.40589-v08816) and the chimeric CCMV CPs. The plates were incubated with the antigen solution for 24 h at 4 °C (200 ng/well for the synthetic peptide; 50 ng/well for both S proteins and CCMV CPs). The incubation buffer consisted of 15 mM Na_2CO_3 and 35 mM $NaHCO_3$). The plates were washed three times with PBS-Tween after each step. The

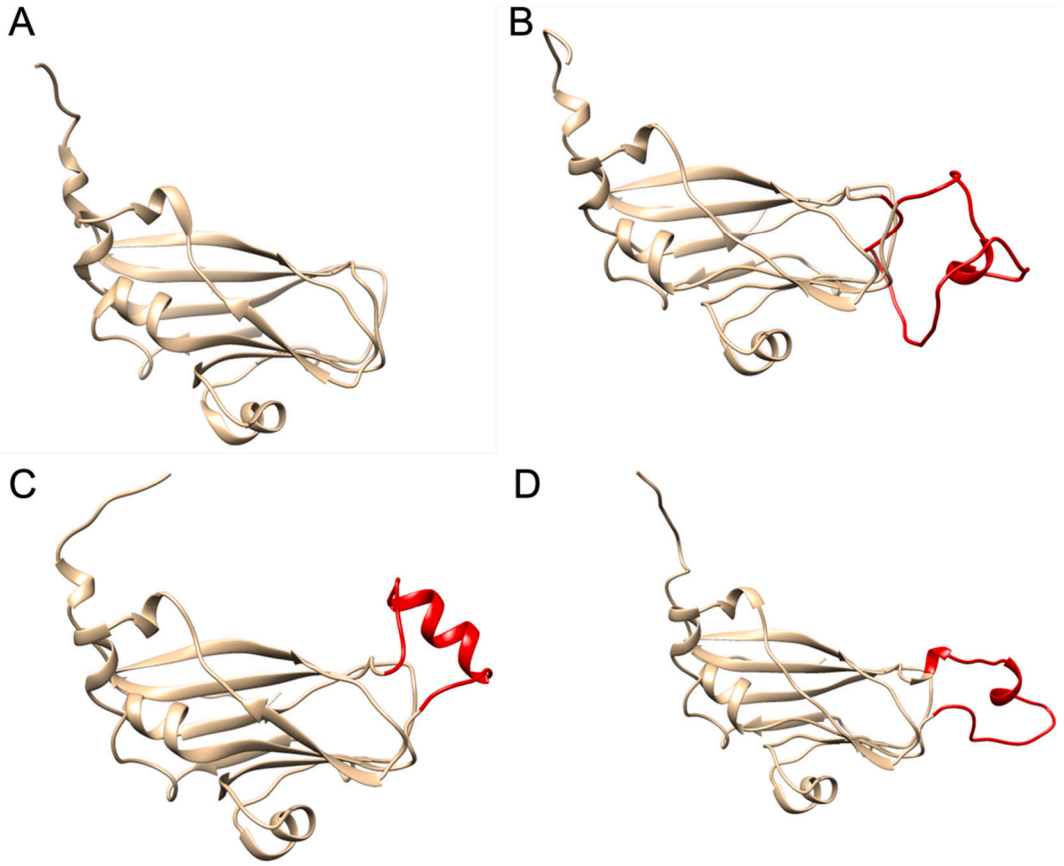

Fig. 2. Modeled 3D structure of the chimeric CCMV/SARS-CoV-2 proteins. A) Crystal structure of the wild-type CCMV CP. B) Predicted structure of the CCMV 1, C) 2, and D) 3 CPs that contain the $S_{462–500}$, $S_{505–522}$, and $S_{439–460}$ epitopes (red), respectively. The prediction was generated using the ProMod3 modeling engine. The in silico analysis does not predict drastic changes in the secondary and tertiary structure of the capsid proteins due to the insertion of the epitopes. (For interpretation of the references to colour in this figure legend, the reader is referred to the web version of this article.)

samples were blocked by incubating the plate for 24 h with 5 % skim milk at 25 °C. Dilution of the test sera was applied to the plate, followed by incubation overnight at 4 °C. As a secondary antibody, a donkey anti-mouse IgG1 with horseradish peroxidase-conjugated antibody was used (1:10,000 dilution, Sigma-Aldrich, St. Louis, MO). An ABTS substrate solution containing 0.6 mM 2,2′-Azino-bis (3-ethylbenzothiazoline-6-sulfonic acid) (ABTS; Sigma-Aldrich), 0.1 M citric acid, and 1 mM H_2O_2 at pH 4; was used for detection of binding antibodies. After a 30 min-incubation at 25 °C, the optical density at 405 nm was recorded with a Multiskan FC microplate photometer (Thermo Fisher Scientific, Waltham, MOM). Statistical analysis comprised ANOVAs ($p < 0.05$) ran in the STATISTICA software version 10 by Stat Soft. Inc.

3. Results

3.1. Design of CCMV-based chimeras carrying S epitopes are efficiently expressed in E. coli

The SARS-CoV-2 epitopes used in the present study were chosen because the RBD is considered a key antigen for the induction of neutralizing antibodies and relevant T cell responses. CCMV1 ($S_{462–500}$) contains six complete and one partial ACE2 binding sites, which represent about half of the ACE2 binding sites, and according to the in silico analysis, one Helper T (Th) cell epitope [21], and one cytotoxic T lymphocyte (CTL) epitope [22]. CCMV2 ($S_{505–522}$) contains one ACE2 binding site, whereas CCMV3 ($S_{439–460}$) contains three ACE2 binding sites, one Th cell epitope, and one CTL epitope. The insertion of the SARS-CoV-2 epitopes into the CCMV CP sequence was determined by finding the most exposed loop between the β-sheets (see Fig. 1). To determine if the insertion of the peptides could completely disrupt the secondary and tertiary structure of the CP, the chimeric protein was modeled using the ProMod3 modeling engine (see Fig. 2). Several insertion sites were assessed until we found that insertion of the epitopes between the CP amino acids 164 and 165 had the least deleterious effects. It is important to note that these simulations do not guarantee that the mutations will not affect the structure of the CP but were used to determine the most likely insertion site from the three loops that preserve the overall integrity of the capsid protein.

3.2. CCMV-based chimeras are efficiently expressed in E. coli

The expression of the CCMV-based chimeras was confirmed by SDS-PAGE, as is shown in Fig. 3. Three colonies transformed with each plasmid were assessed for protein expression in an initial screening. All the analyzed colonies showed the presence of the expected recombinant proteins (22.1, 26.5, 24.2, and 24.8 kDa for WT, CCMV1, CCMV2, and CCMV3, respectively). Based on the relative amount of recombinant protein accumulated by each clone, the following clones were selected for further experiments: WT.1, CCMV 1.1, CCMV2.1, CP CCMV 3.3.

Once the clones WT.1, CCMV 1.1, CCMV 1.2, CP CCMV 1.3 were selected, we proceeded to purify the WT and chimeric proteins. Despite our efforts to use different lysis and solubilization protocols, most recombinant chimeric proteins remain in the insoluble fraction (e.g., inclusion bodies). This is contrary to the WT CP, which in almost every protocol accumulates roughly equal amounts in the soluble and insoluble protein fractions (data not shown). This difference in solubilities suggests that the insertion of the SARS-CoV-2 epitopes can affect the folding of the protein. Therefore, we solubilized the chimeric proteins

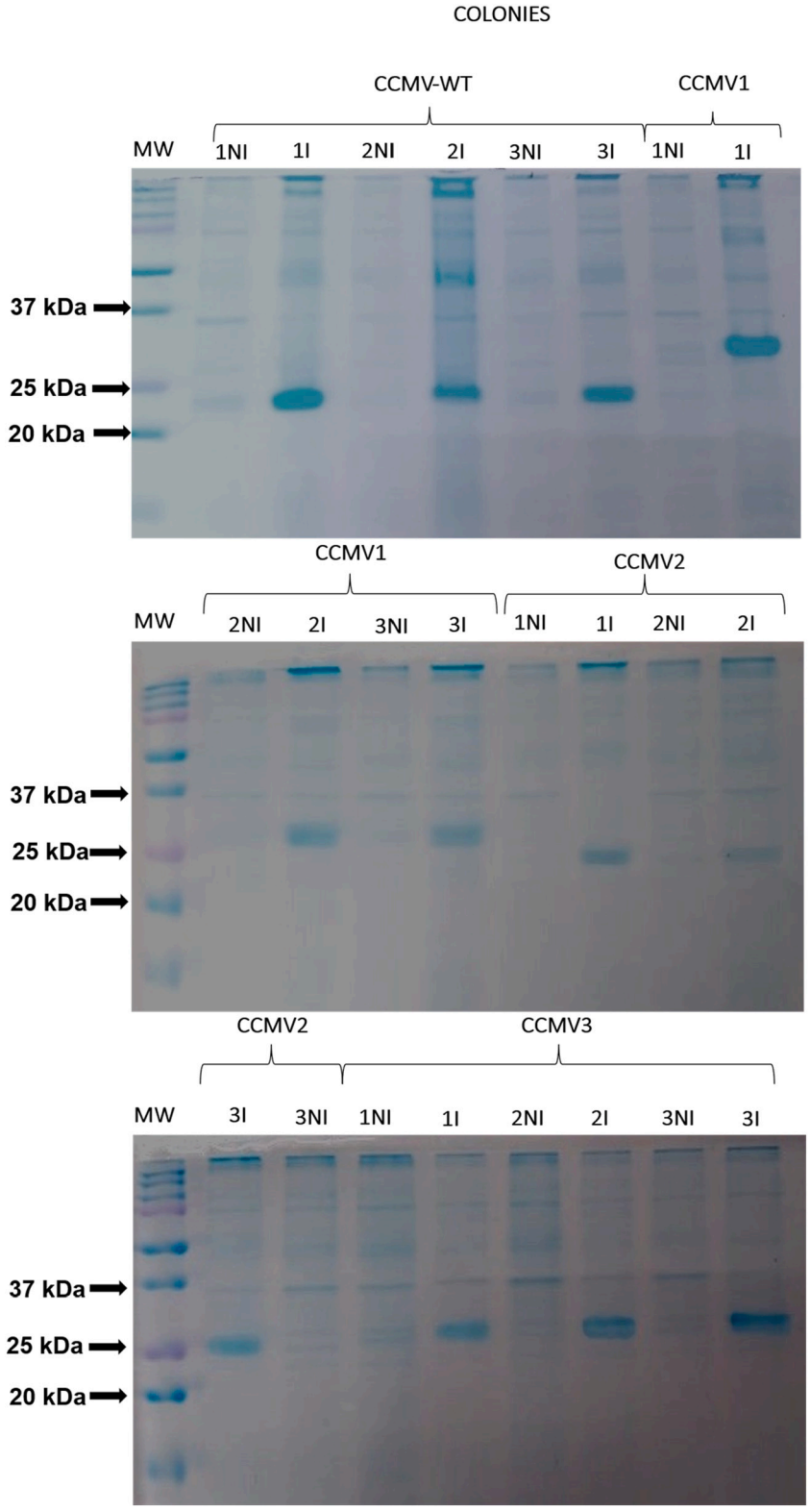

Fig. 3. Expression assessment for the CCMV1-based chimeras carrying S epitopes using recombinant *E. coli* (Rosetta DE3). SDS-PAGE gels for the analysis of clones expressing CCMV CPs (WT, and 1-3 mutants) at the pre-induction (NI) or the post-induction (I) phase. The numbers on the far left correspond to the molecular weight of the protein ladder. The expected molecular weight of the WT and CPs are 22.1, 26.5, 24.2, and 24.8 kDa, respectively.

from the inclusion bodies using denaturing conditions. The protocol that allowed for the highest amount of soluble protein recovered from the inclusion bodies consisted of first washing the insoluble fraction with 2 M urea, 20 mM Tris-HCl, 0.5 M NaCl, 2 % Triton™ X-100 pH 8.0, followed by a series of washes with 20 mM Tris-HCl, 0.5 M NaCl, 5 mM imidazole, 6 M guanidine hydrochloride, and 1 mM 2-mercaptoethanol, pH 8.0, and a final resuspension in 20 mM Tris-HCl, 0.5 M NaCl, 20 mM imidazole, 1 mM 2-mercaptoethanol, 6 M urea, pH 8.0. Fig. 4 A shows the SDS-PAGE of the recombinant proteins recovered in the final resuspension step with the buffer that contains 6 M Urea. The molecular

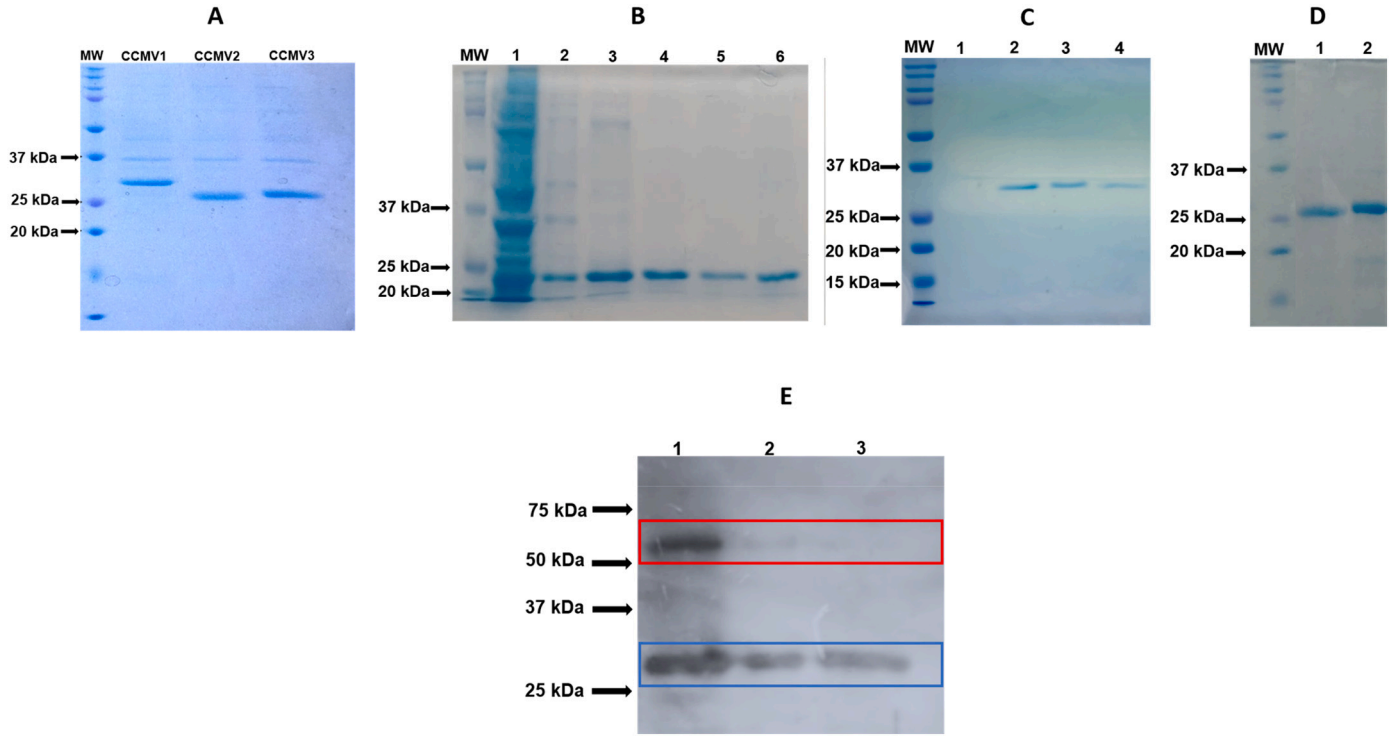

Fig. 4. Data on the purification of CCMV CPs. A) Protein patterns from inclusion bodies are solubilized using a series of washed with denaturing buffers. Most of the endogenous proteins present in the inclusion bodies are removed by the treatment with the buffer containing 6 M Urea. B) C) and D) representative SDS- PAGE gels for the purification by IMAC of CCMV1, CCMV2, and CCMV3, respectively. B) Purification of CCMV WT by nickel resin from soluble fraction, lane 1 shows the fraction not bound to the resin, lane 2: washing the nickel resin with 20 mM imidazole to remove proteins weakly bound to the resin. Lanes 2 and 3: washing the nickel resin with 250 mM imidazole to remove bound proteins moderately bound to the resin. Lanes 4–6 washing the nickel resin with 500 mM imidazole used to elute our protein of interest. C) Purification of CCMV1 by nickel resin from soluble fraction, lane 1: washing the nickel resin with 20 mM imidazole to remove proteins weakly bound to the resin. Lanes 2–4: washing the nickel resin with 500 mM imidazole used to elute our protein of interest (thee elutions). D) Chimeras 2 and 3 after nickel resin purification and elution with 500 mM imidazole. E) Western Blot to assess the antigenicity of the CCMV1 protein using an anti-serum against the SARS-CoV-2 target sequence. The red box shows dimeric CP, and the blue box represents the monomeric protein. (For interpretation of the references to colour in this figure legend, the reader is referred to the web version of this article.)

weight of the most prominent band in each lane corresponds to the expected weights for the chimeric proteins. Furthermore, this analysis shows that the samples contain small amounts of other proteins.

The chimeric and WT CPs have an N-terminal His-tag. Therefore, after solubilization from the inclusion bodies, we refolded the proteins while bound to Ni-NTA beads. This was done by washing the bound protein with Tris-HCl buffers that contain 20 mM imidazole, NaCl, 2-mercaptoethanol, and pH 8 with varying concentrations of urea that range from 6 to 0 M. After refolding the proteins, buffers containing 20 and 250 mM of imidazole were applied to wash out the weakly bound protein and a 500 mM-imidazole containing buffer allowed an efficient elution of the WT CCMV CP, with high purity (Fig. 4-B). Based on these results, the same conditions were applied during the purification of the chimeric CCMV CPs, observing similar yields and purity (see Fig. 4C, D).

3.3. The chimeric CP are recognized by antibodies against the RBD

We have previously reported the generation of hyperimmune sheep serum that recognizes a portion of the RBD. The epitope in CCMV1 falls within the RBD region used to generate the hyperimmune serum; hence we used this serum to determine if RBD-specific antibodies can recognize the refolded CCMV1 protein [20]. Fig. 4-E shows a western blot of the three 500 mM imidazole elutions for CCMV1, as well as the elution with 20 mM imidazole, which contains the non-bound proteins. This blot shows that the epitope in CCMV1 can be recognized by our RBD-specific hyperimmune serum, confirming that the band of interest observed by SDS-PAGE belongs to the chimeric protein. Furthermore, it is well known that in solution, CCMV CP is in a dimeric form [24], and under denaturing conditions, most of the dimers are disrupted. However, Fig. 4-E shows that by Western blot, we can detect that in a fraction of the CCMV1 CP dimers prevail under the denaturing conditions of an SDS-PAGE. The dimerization of WT CCMV CP occurs through the direct interaction between the C-termini of each monomer [25]; therefore, this result suggests that the refolded protein retains at least some of the proper tertiary structure that allows it to dimerize.

Table 1
Description of the treatments assigned to each mice group ($n = 4$) for immunogenicity assessment.

Group	Vaccine
G1	PBS (Negative control)
G2	CCMV1-PBS (10 μg)
G3	CCMV1-Al(OH)$_3$ (10 μg)
G4	CCMV-WT(10 μg)
G5	CCMV2-PBS(10 μg)
G6	CCMV2- Al(OH)$_3$(10 μg)
G7	CCMV3-PBS(10 μg)
G8	CCMV3- Al(OH)$_3$(10 μg)
G9	CCMV1/CCMV2/CCMV3- Al(OH)$_3$(25 μg)

3.4. The CCMV1-3 chimeras induce strong IgG responses in test mice

Table 1 contains the nine different immunization groups. It is important to point out that at least during the immunization protocol, none of the animals died, nor presented abnormal behavior, suggesting that our vaccine candidates are safe (data not shown). Fig. 5 shows the

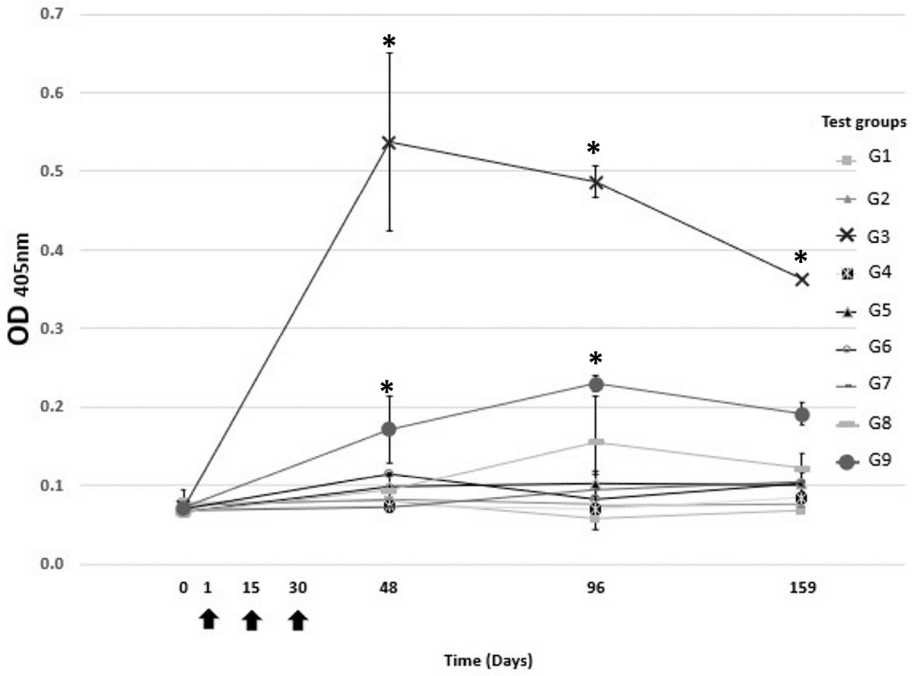

Fig. 5. Levels of total anti-S IgG determined by ELISA. The antigen used was the full-length S protein (Delta variant). The arrows indicate the days of immunization of the mice. G1(Negative group); G2 (CCMV1-PBS (10 μg); G3 CCMV1-Al(OH)$_3$ (10 μg); G4 CCMV-WT(10 μg);G5 CCMV2-PBS(10 μg); G6 CCMV2- Al(OH)$_3$(10 μg); G7 CCMV3-PBS(10 μg); G8 CCMV3- Al(OH)$_3$(10 μg); G9 CCMV1/CCMV2/ CCMV3- Al(OH)$_3$(25 μg). The asterisks denote the statistically significant differences versus the negative control group (G1) at $P < 0.05$.

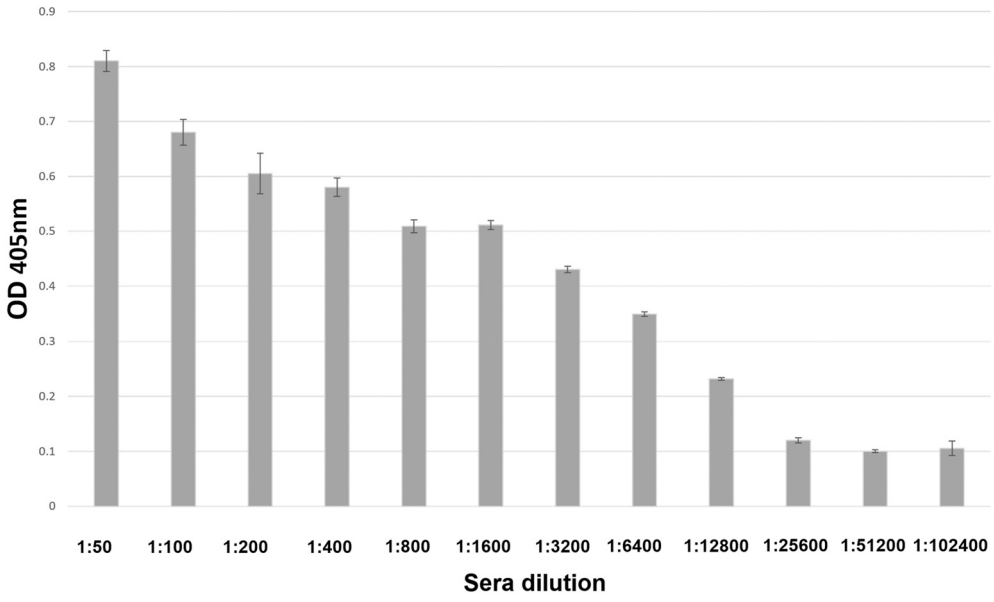

Fig. 6. ELISA-based detection of anti-S IgG in serial dilutions of sera from mice immunized with CCMV1 + adjuvant. The antigen used was the full-length S protein. The error bars are the standard deviation of the mean absorbance value from the four mice per group. The total IgG antibody titers in this group were 12,800. The serum was collected 66 days after the third immunization. The error bars are the standard deviation of the mean absorbance value from the four mice per group.

results of the indirect ELISA performed to measure IgG response in sera samples (1:800 dilution) taken 18 days after the third immunization. In this case, the target antigen was the full-length S protein from the Wuhan sequence. The group immunized with CCMV1 plus the adjuvant (G3) showed the highest antibody titers 18 days after the immunization protocol was completed compared to all other groups. Groups 8 and 9 (CCMV3 + adjuvant, and CCMV1 + CCMV2 + CCMV3 + adjuvant, respectively) had similar immunogenic properties; however, they were considerably lower than for G3. This suggests that the formulation comprising adjuvanted CCMV1 induces a better immune response than the other vaccine candidates and that CCMV1 is the most promising antigen in terms of inducing antibodies with a robust capacity to bind the native viral target. Thus, we focused all further efforts on better characterizing the immunogenicity of CCMV1 with adjuvant. Fig. 6 shows the ELISA with serial dilutions of the serum from G3 and was used to determine the total IgG antibody titers produced by this antigen. The total IgG antibody titers for this group were 12,800.

To further characterize the immunogenicity of CCMV1 + adjuvant, we measured the relative levels of the IgG subclasses IgG1 and IgG2a in the G3 group; observing higher level of IgG1 in both G3 and G9, with a higher response in G3 compared to G9 (Fig. 7).

In the previous ELISAs we used the full-length S protein as the antigen; however, we wanted to investigate whether we could use a synthetic peptide covering 31 of the 38 amino acids that constitute the

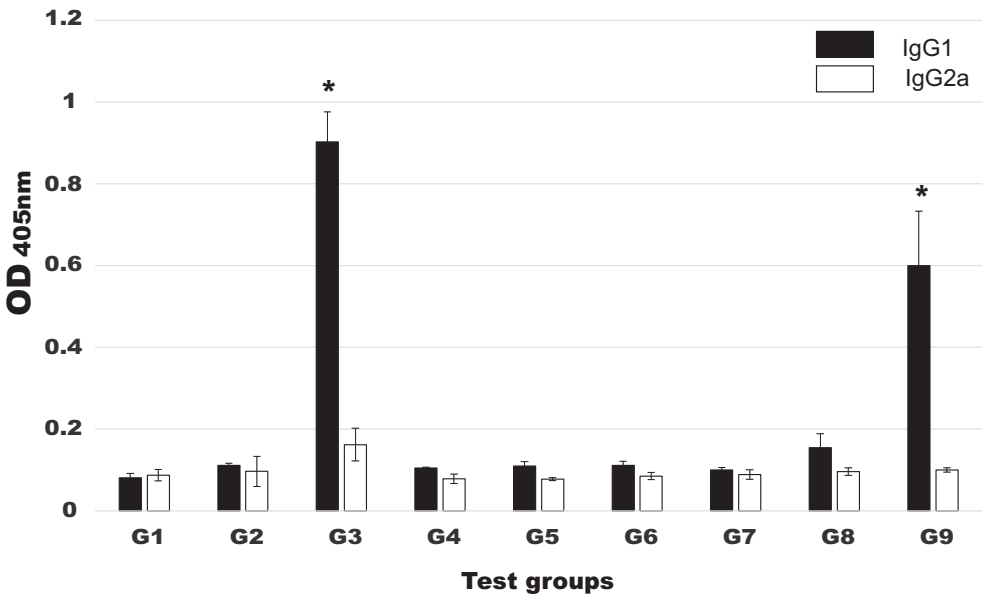

Fig. 7. Levels of anti-S IgG subclasses determined by ELISA. The antigen used was the full-length S protein. The sera were diluted to 1:1600. G1(negative group); G2 (CCMV1-PBS (10 μg); G3 CCMV1-Al$(OH)_3$ (10 μg);G4 CCMV-WT(10 μg);G5 CCMV2-PBS(10 μg); G6 CCMV2- Al$(OH)_3$(10 μg); G7 CCMV3-PBS(10 μg); G8 CCMV3- Al$(OH)_3$(10 μg); G9 CCMV1/CCMV2/CCMV3- Al $(OH)_3$(25 μg). The error bars are the standard deviation of the mean absorbance value for each experimental group. The asterisks denote the statistically significant differences versus the IgG2a mean signal at $P < 0.05$.

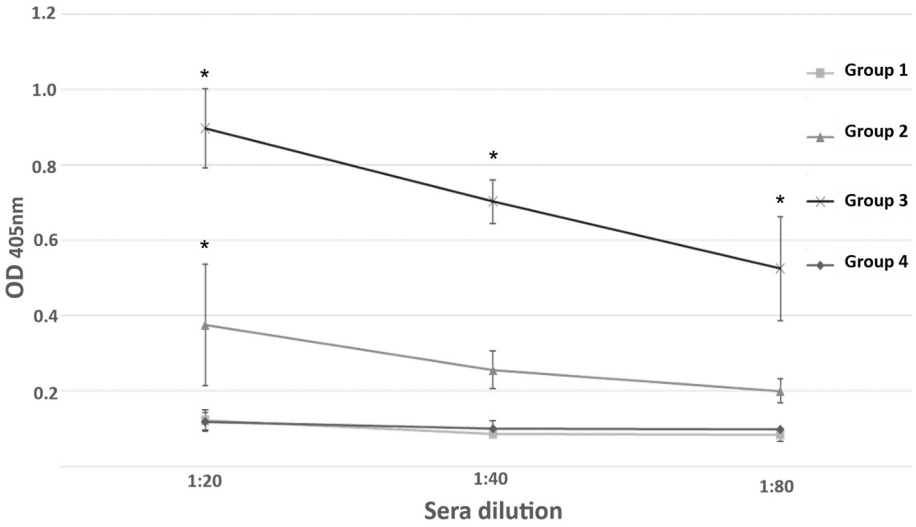

Fig. 8. Levels of anti-$S_{461–493}$ IgG antibodies determined by ELISA. Sera was obtained from the following groups: G1 (Negative group); G2 (CCMV1-PBS (10 μg); G3 CCMV1-Al$(OH)_3$ (10 μg); and G4 CCMV-WT(10 μg); and analyzed by ELISA using the peptide $S_{461–493}$ as the target antigen. The asterisks denote the statistically significant differences versus the negative control group (G1) at $P < 0.05$.

SARS-CoV-2 epitope in CCMV1 as an antigen to detect the antibodies generated by these vaccine candidates. Fig. 8 shows the indirect ELISA for different sera dilutions for G1, G2, G3, and G4, where the antigen used was a synthetic peptide covering $S_{461–493}$. This antigen was able to modestly detect antibodies of the mice immunized with CCMV1 without adjuvants (G2). The detection of the antibodies generated by CCMV1 + adjuvant was higher than for G2. As expected, this ELISA did not detect the antibodies generated by mice with the mock immunization (G1) or those immunized with the WT CCMV. The drastic loss of sensibility in this ELISA suggests that the lack of tertiary structure in the peptide, compared to the full-length protein, negatively affects the recognition of antibodies generated with a "structured" version of the same peptide.

The binding capacity of the antibodies induced by the CCMV CP chimeras was also determined using the S protein from the Delta variant. As shown in Fig. 9, the binding capacity of the CCMV1-induced antibodies to the Delta variant S protein was lower (two-fold) compared to that of the Wuhan S protein, which is expected as the Delta variant carries one point mutation in the target epitope present in CCMV1 (T478K).

An anti CP-ELISA revealed that animals seroconverted after the first boost (data not shown), indicating the induction of antibodies against the carrier. However, as mentioned above, the anti-S response was magnified by the CCMV1 antigen upon further boostings, suggesting that the anti-CP antibodies do not block the production of anti-RBD antibodies.

4. Discussion

In the present study, chimeric CCMV-based proteins were produced as attractive immunogens against SARS-CoV-2. Plants viruses can be a highly advantageous platform for producing biopharmaceuticals; they can be produced either in plants or in recombinant systems (e.g., *E. coli*); thus, they can become low-cost production systems. Furthermore, they can be easily genetically and/or chemically modified to present novel epitopes. Therefore, they should be explored as a platform for generating vaccines and immunomodulant molecules. In addition, structure

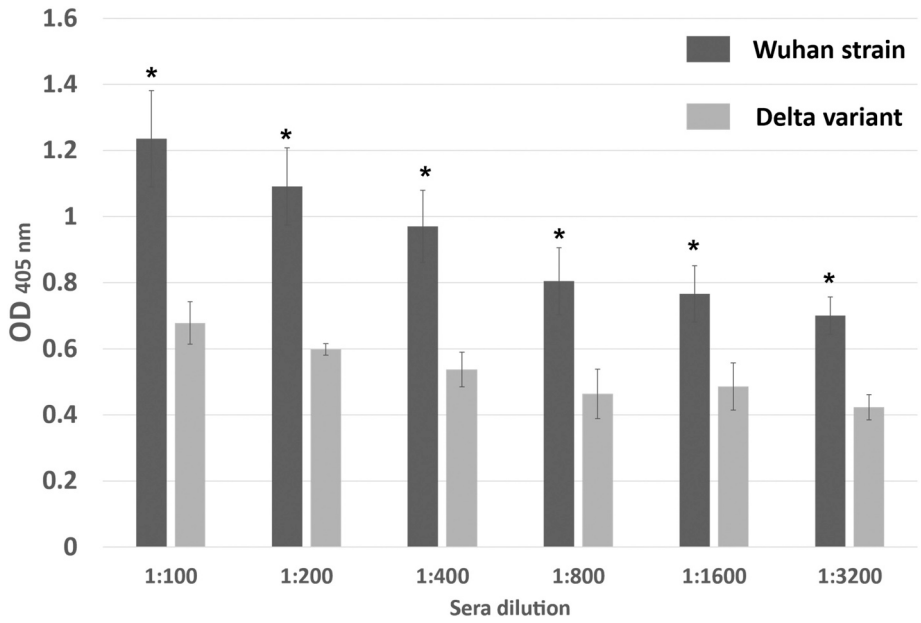

Fig. 9. Levels of anti-S IgG antibodies determined by ELISA. Sera from mice immunized with CCMV1-AL(OH)$_3$ (G3) was analyzed by ELISA using Delta variant- or Wuhan- S protein as the target antigen. The error bars are the standard deviation of the mean absorbance value from the four mice. The asterisks denote the statistically significant differences versus the signal of the anti-Delta response at $P < 0.05$.

and epitope-based vaccine design has become a promising strategy to improve the efficacy of subunit vaccines [23], and the intrinsic properties of the plant viruses can be used for the generation of novel subunit vaccines that could have a higher immunogenic profile when fused to the antigen of interest that when administered alone. In other words, the viral component of the subunit vaccine could act as a carrier/adjuvant. This is especially important in the context of the low immunogenicity that most subunit vaccines have when presented without the appropriate adjuvants.

In this article, we genetically engineered the CP of CCMV to deliver different SARS-CoV-2 epitopes from the S protein, which is critical to achieving immunoprotection against COVID-19. As a first effort, we decided to use the CP in its dimeric form rather than as a virus-like-particle (VLPs) that contains 180 CP with icosahedral symmetry. The choice of using the CP in its dimeric form was primarily motivated by the fact that recombinant protein went to the inclusion bodies. Nonetheless, we are optimizing the expression system to purify soluble CP and thus immunize mice with VLPs rather than the dimeric CP. Furthermore, the goal to purify the chimeric CCMV/SARS-CoV-2 VLPs is further motivated by the modest antibody titers observed in the immunized groups that do not contain the adjuvant.

Of the three chimeric CPs, CCMV1 is considered the most promising one since it induced higher IgG levels targeting the native S protein. CCMV1 contains the $S_{463–500}$ epitope, which carries a Th and a CTL epitope, as well as six ACE2 binding sites. Therefore, this mutant will be next evaluated in the form of VLPs to determine if it is able to induce such a humoral response in the absence of adjuvants.

An issue of concern is the effectiveness of the current vaccines against the current VOC (e.g., Delta and Omicron) and any future variants. For example, studies have revealed that the variant B.1.617.2 evades neutralizing antibodies from sera of convalescent patients, as well as sera from individuals vaccinated with two different vaccines, one based on an adenovirus vector (ChAdOx1) and the other mRNA based (BNT162b2) [26]. However, the BNT162b2 and mRNA-1273 vaccines both showed robust effectiveness (≥90 %) against Delta-related hospitalization and fatality, in line with studies from the United Kingdom, United States, and Israel [27]. Furthermore, after the completion of the two-shot Pfizer vaccine, the rate of protection against the Delta variant was 79–87 %, while that of the AstraZeneca vaccine was 60 %, both of which were lower than those against the Alpha variant [28]. These results are consistent with our findings. On the one hand, the epitope in CCMV1 has only one mutation with respect to the Delta variant (T478K), and this was enough to decrease the ability of the CCMV1-induced antibodies to recognize the S protein from the Delta variant. These results clearly show that antibody-antigen binding is greatly influenced by the binding site and its surrounding structural context.

Our study suggests that using genetically engineering CCMV CP to present three different SARS-CoV-2 epitopes from protein S is a potential option for creating an effective vaccine against COVID-19. Previous studies have shown that this protein, under suitable pH conditions, forms VLPs and other non-canonical structures [16]. The ability of plant viruses such as CCMV and brome mosaic virus (BMV) [29] to self-assemble in the presence and absence of nucleic acid as well as in different shapes can become an advantage to produce chimeric proteins that present multiple copies of the antigen of interest, which could decrease the need of using adjuvants. Furthermore, an important consideration is that plant virus nanotechnologies offer high thermal stability [30]; CCMV VLPs can be stable at temperatures between −80 and 50 °C, thus overcoming the need for cold-chain storage and distribution [31]. This is a clear advantage over the vaccine platforms already approved today, such as mRNA vaccines. Another advantage of the CCMV-based platform is related to the detrimental effect on the vaccine efficacy induced by blocking antibodies. Upon immunization anti-CP antibodies will be indeed induced, as shown in the anti-CP ELISA data. However, our results showed that the second and third immunizations induced a dramatic increase in antibody levels supporting the effectiveness of the boost using the CP-based antigens. Another key fact is that CCMV does not infect edible plants for human consumption, and thus vaccinees are not expected to have anti-CP antibodies at the priming phase, maximizing the action of the vaccine; which contrasts with the case of adenoviral vaccines in which the preexisting antibodies may exist as a consequence of possible previous adenovirus infections [32,33].

The evaluation of the neutralizing potential of the antibodies induced by the CCMV-based chimeras is ongoing, using an in-house neutralization assay based on a pseudovirus. RBD-specific antibodies have greater potency to neutralize infection with divergent virus strains [34], however studies on previous SARS-CoV-2 variants have

demonstrated that mutations within the receptor-binding domain (RBD) mediate escape from vaccine-induced neutralizing antibodies [35,36].

The CCMV1 chimera showed a sufficient immune response against the Delta variant, although lower than that against Wuhan S protein. However, the response against the Omicron variant remains to be evaluated since Omicron has 15 mutations in the RBD region of the spike protein, of which six falls into the CCMV1 sequence (E484A, S477N, T478K, Q493R, G496S, and Q498Y). Given the 15 mutations present in the RBD of Omicron, it was anticipated that this variant would be significantly associated with immune evasion [35,37]. In fact, there is evidence showing that Omicron could lead to a 10–40-fold reduction in neutralization capacity [38].

Previous studies agree that the costs of cultivating *E. coli* are 10- to 100-fold less expensive than those implied for growing non-microbial eukaryotic cells [39]. The expression of RBD in *E. coli* has been explored by some groups; however, this recombinant protein is largely insoluble and therefore requires solubilization and refolding [40], perhaps due to the incompatibility between the four disulfide bonds in the native RBD structure and the reducing environment of the *E. coli* cytoplasm [41]. Our CCMV-based chimeras were easily solubilized and resulted in stable proteins, rendering a highly promising platform for producing epitope-based vaccines against SARS-CoV-2. Biomass yields ranged 14-15.15 g/L whereas recombinant protein yield was 750 μg/L on average, which is lower to other studies reporting biomass yields of 28 g/L and recombinant protein yields of 122 mg/L [39].

Mice and humans have several IgG isotypes that differ in their ability to recruit innate cells, fix complements, and engage Fcγ-receptors [40]. When BALB/c mice mount a Th2 response, IgG1 is predominantly produced, while Th1 responses comprise predominant IgG2a antibodies [42]. Interestingly, the immune response induced by the test chimeras comprised the IgG1 subclass predominantly, suggesting a Th2-biased response, offering an interesting perspective for evaluating the neutralizing potential of the induced antibodies.

In most studies, the vaccine efficacy or effectiveness against severe disease remained high (≥70 %) for up to 6 months after vaccination for Pfizer–BioNTech, Moderna-mRNA, Janssen-Ad26.COV2·S and AstraZeneca-Vaxzevria (and mostly ≥80 % for the two mRNA vaccines) [43]. The monitoring of the acquired immunity with the chimeras was carried out up to 4 months after the last dose administered to the mice, showing a favorable response even to high serum titers for CCMV1 with adjuvant. A point to consider is that the waning protection against infection over time was due to both declining immunity and the emergence of variants [44,45].

CRediT authorship contribution statement

Claudia Almendárez-Rodriguez: Methodology, Conceptualization, Validation, Writing - Original Draft. **Karla I. Solis-Andrade:** Methodology. **Dania O. Govea-Alonso:** Methodology. **Mauricio Comas-Garcia:** Conceptualization, Investigation, Writing - Review & Editing, Supervision.**Sergio Rosales-Mendoza:** Conceptualization, Investigation, Writing - Review & Editing, Supervision, Project administration, Funding acquisition.

Acknowledgements

This work was supported by Consejo Nacional de Ciencia y Tecnología (CONACyT, grants C-146/2021 and 848290 to S R-M; MSc studies' fellowship to C A-R, CVU 1031199).

References

[1] Coronaviridae Study Group of the International Committee on Taxonomy of Viruses, The species Severe acute respiratory syndrome-related coronavirus: classifying 2019-nCoV and naming it SARS-CoV-2, Nat. Microbiol. 5 (4) (2020) 536–544, https://doi.org/10.1038/s41564-020-0695-z.

[2] K. Rawat, P. Kumari, L. Saha, COVID-19 vaccine: a recent update in pipeline vaccines, their design and development strategies, Eur. J. Pharmacol. 892 (2021), 173751, https://doi.org/10.1016/j.ejphar.2020.173751.

[3] D. Martínez-Flores, J. Zepeda-Cervantes, A. Cruz-Reséndiz, S. Aguirre-Sampieri, A. Sampieri, L. Vaca, SARS-CoV-2 vaccines based on the spike glycoprotein and implications of new viral variants, Front. Immunol. 12 (2021), 701501, https://doi.org/10.3389/fimmu.2021.701501.

[4] J. Yang, W. Wang, Z. Chen, et al., A vaccine targeting the RBD of the S protein of SARS-CoV-2 induces protective immunity, Nature 586 (2020) 572–577, https://doi.org/10.1038/s41586-020-2599-8.

[5] S. Alexandersen, A. Chamings, T.R. Bhatta, SARS-CoV-2 genomic and subgenomic RNAs in diagnostic samples are not an indicator of active replication, Nat. Commun. 11 (2020) 6059, https://doi.org/10.1038/s41467-020-19883-7.

[6] R. Sanjuán, P. Domingo-Calap, Mechanisms of viral mutation, Cell. Mol. Life Sci. 73 (23) (2016) 4433–4448, https://doi.org/10.1007/s00018-016-2299-6.

[7] J.Y. Choi, D.M. Smith, SARS-CoV-2 variants of concern, Yonsei Med. J. 62 (11) (2021) 961–968, https://doi.org/10.3349/ymj.2021.62.11.961.

[8] J. Chen, R. Wang, N.B. Gilby, G.W. Wei, Omicron (B.1.1.529): Infectivity, Vaccine Breakthrough, and Antibody Resistance, ArXiv, 2021 arXiv:2112.01318v1.

[9] Hui-Yao Huang, Yu. Shu-Hang Wang, Wei Sheng Tang, Chi-Jian Zuo, Wu. Da-Wei, Hong Fang, Du. Qiong, Ning Li, Landscape and progress of global COVID-19 vaccine development, Hum. Vaccin. Immunother. 17 (10) (2021) 3276–3280, https://doi.org/10.1080/21645515.2021.1945901.

[10] L. Du, Y. He, S. Jiang, B.J. Zheng, Development of subunit vaccines against severe acute respiratory syndrome, Drugs Today 44 (2008) 63–73, https://doi.org/10.1358/dot.2008.44.1.1131830.

[11] M. Verdecia, J.F. Kokai-Kun, M. Kibbey, S. Acharya, J. Venema, F. Atouf, COVID-19 vaccine platforms: delivering on a promise? Hum. Vaccin. Immunother. 17 (9) (2021) 2873–2893, https://doi.org/10.1080/21645515.2021.1911204.

[12] A. Singh, G. Kaur, S. Singh, N. Singh, G. Saxena, P.C. Verma, Recombinant plant engineering for immunotherapeutic production, Curr. Mol. Biol. Rep. 3 (4) (2017) 306–316, https://doi.org/10.1007/s40610-017-0078-2.

[13] P. Lam, N.F. Steinmetz, Delivery of siRNA therapeutics using cowpea chlorotic mottle virus-like particles, Biomater. Sci. 7 (8) (2019) 3138–3142, https://doi.org/10.1039/c9bm00785g.

[14] S. Zinkhan, A. Ogrina, I. Balke, G. Reseviča, A. Zeltins, S. de Brot, C. Lipp, X. Chang, L. Zha, M. Vogel, M.F. Bachmann, M.O. Mohsen, The impact of size on particle drainage dynamics and antibody response, J. Control. Release 331 (2021) 296–308, https://doi.org/10.1016/j.jconrel.2021.01.012.

[15] S. Timmermans, D. Vervoort, L. Schoonen, R. Nolte, J. van Hest, Self-assembly and stabilization of hybrid cowpea chlorotic mottle virus particles under nearly physiological conditions, Chem. Asian J. 13 (22) (2018) 3518–3525, https://doi.org/10.1002/asia.201800842.

[16] A. Hassani-Mehraban, S. Creutzburg, L. van Heereveld, R. Kormelink, Feasibility of cowpea chlorotic mottle virus-like particles as scaffold for epitope presentations, BMC Biotechnol. 15 (2015) 80, https://doi.org/10.1186/s12896-015-0180-6.

[17] A. Díaz-Valle, Y.M. García-Salcedo, G. Chávez-Calvillo, L. Silva-Rosales, M. Carrillo-Tripp, Highly efficient strategy for the heterologous expression and purification of soluble cowpea chlorotic mottle virus capsid protein and in vitro pH-dependent assembly of virus-like particles, J. Virol. Methods 225 (2015) 23–29, https://doi.org/10.1016/j.jviromet.2015.08.023.

[18] R.F. Garmann, M. Comas-Garcia, M.S. Koay, J.J. Cornelissen, C.M. Knobler, W. M. Gelbart, Role of electrostatics in the assembly pathway of a single-stranded RNA virus, J. Virol. 88 (18) (2014) 10472–10479, https://doi.org/10.1128/JVI.01044-14.

[19] L. Lavelle, J.P. Michel, M. Gingery, The disassembly, reassembly and stability of CCMV protein capsids, J. Virol. Methods 146 (1–2) (2007) 311–316, https://doi.org/10.1016/j.jviromet.2007.07.020.

[20] 1 S. Farfán-Castro, M.J. García-Soto, M. Comas-García, J.I. Arévalo-Villalobos, G. Palestino, O. González-Ortega, S. Rosales-Mendoza, Synthesis and immunogenicity assessment of a gold nanoparticle conjugate for the delivery of a peptide from SARS-CoV-2, Nanomedicine 34 (2021), 102372, https://doi.org/10.1016/j.nano.2021.102372.

[21] A. Grifoni, J. Sidney, Y. Zhang, R.H. Scheuermann, B. Peters, A. Sette, A sequence homology and bioinformatic approach can predict candidate targets for immune responses to SARS-CoV-2, Cell Host Microbe 27 (4) (2020) 671–680, https://doi.org/10.1016/j.chom.2020.03.002, e2.

[22] S. Kimar, V.K. Maurya, A.K. Prasad, M. Bhatt, S.K. Saxena, Structural, glycosylation and antigenic variation between 2019 novel coronavirus (2019-nCoV) and SARS coronavirus (SARS-CoV), Virusdisease 31 (1) (2020) 13–21, https://doi.org/10.1007/s13337-020-00571-5.

[23] M. Bhattacharya, A.R. Sharma, P. Patra, P. Ghosh, G. Sharma, B.C. Patra, S.S. Lee, C. Chakraborty, Development of epitope-based peptide vaccine against novel coronavirus 2019 (SARS-COV-2): immunoinformatics approach, J. Med. Virol. 92 (6) (2020) 618–631, https://doi.org/10.1002/jmv.25736.

[24] L. Lavelle, M. Gingery, M. Phillips, W.M. Gelbart, C.M. Knobler, R.D. Cadena-Nava, J.R. Vega-Acosta, L.A. Pinedo-Torres, J. Ruiz-Garcia, Phase diagram of self-assembled viral capsid protein polymorphs, J. Phys. Chem. B 113 (12) (2009) 3813–3819, https://doi.org/10.1021/jp8079765.

[25] J.A. Speir, S. Munshi, G. Wang, T.S. Baker, J.E. Johnson, Structures of the native and swollen forms of cowpea chlorotic mottle virus determined by X-ray crystallography and cryo-electron microscopy, Structure 3 (1) (1995) 63–78.

[26] P. Mlcochova, S.A. Kemp, M.S. Dhar, G. Papa, B. Meng, I. Ferreira, R. Datir, D. A. Collier, A. Albecka, S. Singh, R. Pandey, J. Brown, J. Zhou, N. Goonawardane, S. Mishra, C. Whittaker, T. Mellan, R. Marwal, M. Datta, S. Sengupta, R.K. Gupta,

SARS-CoV-2 B.1.617.2 Delta variant replication and immune evasion, Nature 599 (7883) (2021) 114–119, https://doi.org/10.1038/s41586-021-03944-y.
[27] P. Tang, M.R. Hasan, H. Chemaitelly, et al., BNT162b2 and mRNA-1273 COVID-19 vaccine effectiveness against the SARS-CoV-2 Delta variant in Qatar, Nat. Med. 27 (2021) 2136–2143, https://doi.org/10.1038/s41591-021-01583-4.
[28] L. Bian, Q. Gao, F. Gao, Q. Wang, Q. He, X. Wu, Q. Mao, M. Xu, Z. Liang, Impact of the Delta variant on vaccine efficacy and response strategies, Expert Rev. Vaccines 20 (10) (2021) 1201–1209, https://doi.org/10.1080/14760584.2021.1976153.
[29] A. Nuñez-Rivera, P. Fournier, D.L. Arellano, A.G. Rodriguez-Hernandez, R. Vazquez-Duhalt, R.D. Cadena-Nava, Brome mosaic virus-like particles as siRNA nanocarriers for biomedical purposes, Beilstein J. Nanotechnol. 11 (2020) 372–382, https://doi.org/10.3762/bjnano.11.28.
[30] M. Hema, G.P.Vishnu Vardhan, H.S. Savithri, M.R.N. Murthy, in: Chapter 6 - Emerging Trends in the Development of Plant Virus-Based Nanoparticles and Their Biomedical Applications, 2019, pp. 61–82, https://doi.org/10.1016/B978-0-12-816328-3.00006-4. ISBN 9780128163283.
[31] O.A. Ortega-Rivera, S. Shukla, M.D. Shin, A. Chen, V. Beiss, M.A. Moreno-Gonzalez, Y. Zheng, A.E. Clark, A.F. Carlin, J.K. Pokorski, N.F. Steinmetz, Cowpea mosaic virus nanoparticle vaccine candidates displaying peptide epitopes can neutralize the severe acute respiratory syndrome coronavirus, ACS Infect. Dis. 7 (11) (2021) 3096–3110, https://doi.org/10.1021/acsinfecdis.1c00410.
[32] A.M. Leen, et al., Identification of hexon-specific CD4 and CD8 T-cell epitopes for vaccine and immunotherapy, J. Virol. 82 (2008) 546–554.
[33] S.A. Mendonça, R. Lorincz, P. Boucher, D.T.N.P.J. Curiel, Adenoviral vector vaccine platforms in the SARS-CoV-2 pandemic, Vaccines 6 (1) (2021 Aug 5) 97, https://doi.org/10.1038/s41541-021-00356-x.
[34] S. Jiang, C. Hillyer, L. Du, Neutralizing antibodies against SARS-CoV-2 and other human coronaviruses, Trends Immunol. 41 (5) (2020) 355–359, https://doi.org/10.1016/j.it.2020.03.007.
[35] W.F. Garcia-Beltran, K.J. St Denis, A. Hoelzemer, E.C. Lam, A.D. Nitido, M. L. Sheehan, C. Berrios, O. Ofoman, C.C. Chang, B.M. Hauser, J. Feldman, A. L. Roederer, D.J. Gregory, M.C. Poznansky, A.G. Schmidt, A.J. Iafrate, V. Naranbhai, A.B. Balazs, mRNA-based COVID-19 vaccine boosters induce neutralizing immunity against SARS-CoV-2 omicron variant, Cell 185 (3) (2022) 457–466, https://doi.org/10.1016/j.cell.2021.12.033. Ai, J., Zhang, H.
[36] Y. Zhang, K. Lin, Y. Zhang, J. Wu, Y. Wan, Y. Huang, J. Song, Z. Fu, H. Wang, J. Guo, N. Jiang, M. Fan, Y. Zhou, Y. Zhao, Q. Zhang, Q. Liu, J. Lv, P. Li, W. Zhang, Omicron variant showed lower neutralizing sensitivity than other SARS-CoV-2 variants to immune sera elicited by vaccines after boost, Emerg. Microbes Infect. 11 (1) (2022) 337–343, https://doi.org/10.1080/22221751.2021.2022440.
[37] E. Cameroni, J.E. Bowen, L.E. Rosen, et al., Broadly neutralizing antibodies overcome SARS-CoV-2 omicron antigenic shift, Nature 602 (2022) 664–670, https://doi.org/10.1038/s41586-021-04386-2.
[38] J. Ai, H. Zhang, Y. Zhang, K. Lin, Y. Zhang, J. Wu, Y. Wan, Y. Huang, J. Song, Z. Fu, H. Wang, J. Guo, N. Jiang, M. Fan, Y. Zhou, Y. Zhao, Q. Zhang, Q. Liu, J. Lv, P. Li, W. Zhang, Omicron variant showed lower neutralizing sensitivity than other SARS-CoV-2 variants to immune sera elicited by vaccines after boost, Emerg. Microbes Infect. 11 (1) (2022) 337–343, https://doi.org/10.1080/22221751.2021.2022440.
[39] B.E. McGuire, J.E. Mela, V.C. Thompson, L.R. Cucksey, C.E. Stevens, R. L. McWhinnie, D. Winkler, S. Pelech, F.E. Nano, Escherichia coli recombinant expression of SARS-CoV-2 protein fragments, Microb. Cell Factories 21 (1) (2022) 21, https://doi.org/10.1186/s12934-022-01753-0.
[40] F. Nimmerjahn, J.V. Ravetch, Fc-receptors as regulators of immunity, Adv. Immunol. 96 (2007) 179–204.
[41] G.A. Fitzgerald, A. Komarov, A. Kaznadzey, I. Mazo, M.L. Kireeva, Expression of SARS-CoV-2 surface glycoprotein fragment 319–640 in E coli, and its refolding and purification, Protein Expr. Purif. 183 (2021), 105861.
[42] M.L. Bellone, A. Puglisi, F. Dal Piaz, A. Hochkoeppler, Production in Escherichia coli of recombinant COVID-19 spike protein fragments fused to CRM197, Biochem. Biophys. Res. Commun. 558 (2021) 79–85.
[43] X. Liu, X. Chang, D. Rothen, M. Derveni, P. Krenger, S. Roongta, E. Wright, M. Vogel, K. Tars, M.O. Mohsen, M.F. Bachmann, AP205 VLPs based on dimerized capsid proteins accommodate RBM domain of SARS-CoV-2 and serve as an attractive vaccine candidate, Vaccines 9 (4) (2021) 403, https://doi.org/10.3390/vaccines9040403.
[44] D.R. Feikin, M.M. Higdon, L.J. Abu-Raddad, N. Andrews, R. Araos, Y. Goldberg, M. J. Groome, A. Huppert, K.L. O'Brien, P.G. Smith, A. Wilder-Smith, S. Zeger, M. Deloria Knoll, M.K. Patel, Duration of effectiveness of vaccines against SARS-CoV-2 infection and COVID-19 disease: results of a systematic review and meta-regression, Lancet (London, England) 399 (10328) (2022) 924–944, https://doi.org/10.1016/S0140-6736(22)00152-0.
[45] D.Y. Lin, Y. Gu, B. Wheeler, H. Young, S. Holloway, S.K. Sunny, Z. Moore, D. Zeng, Effectiveness of Covid-19 vaccines over a 9-month period in North Carolina, N. Engl. J. Med. (2022), https://doi.org/10.1056/NEJMoa2117128 arXiv: 2112.01318v1.